

Short communication

Fabrication and characteristics of anode-supported flat-tube solid oxide fuel cell

Jong-Hee Kim^{a,b}, Rak-Hyun Song^{a,*}, Keun-Suk Song^a, Sang-Hoon Hyun^b,
Dong-Ryul Shin^a, Harumi Yokokawa^c

^a Advanced Fuel Cell Research Team, Korea Institute of Energy Research, 71-2 Jang-dong, Yusong-ku, Daejeon 305-343, South Korea

^b Department of Ceramic Engineering, Yonsei University, Seoul 120-749, South Korea

^c Energy Electronics Institute, National Institute of Advanced Industrial Science and Technology, Higashi 1-1-1, Central No. 5, Tsukuba, Japan

Received 6 January 2003; accepted 24 February 2003

Abstract

An anode-supported flat-tube solid oxide fuel cell (SOFC) is developed to increase the cell power density and thermal stability by combining tubular and planar cell structures. The anode-supported flat tube is fabricated by an extrusion process. The porosity and pore size of the Ni/YSZ (8 mol% yttria-stabilized zirconia) cermet anode are 50.6% and 0.23 μm , respectively. The Ni particles are distributed uniformly and are well connected to each other in the cermet. An electrolyte of YSZ and a multi-layered cathode of a $(\text{La}_{0.85}\text{Sr}_{0.15})_{0.9}\text{MnO}_3$ (LSM)/YSZ composite, LSM, and $\text{La}_{0.6}\text{Sr}_{0.4}\text{Co}_{0.2}\text{Fe}_{0.8}\text{O}_3$ (LSCF) are coated on the anode tube by slurry dip coating. The anode-supported flat-tube cell produces 225 mW cm^{-2} (0.6 V, 375 mA cm^{-2}) at 750°C . A ceramic interconnect for the cell stack, $\text{La}_{0.75}\text{Ca}_{0.27}\text{CrO}_3$ (LCC), is synthesized by the Pechini method and is coated on the anode substrate by a plasma spray. A dense layer is obtained. A metallic interconnection plate of Fe–16Cr alloy is coated with LSM by a slurry dip coating process and sintered in a $\text{Ar} + 10\% \text{ H}_2$ atmosphere. The resistance of the LSM-coated alloy is $148 \text{ m}\Omega \text{ cm}^2$ at 750°C and decreases to $43 \text{ m}\Omega \text{ cm}^2$ after 450 h. © 2003 Elsevier Science B.V. All rights reserved.

Keywords: Anode-supported flat tube; Slurry dip coating; Ceramic interconnect; Metallic interconnect; Plasma spray coating; Solid oxide fuel cell

1. Introduction

Solid oxide fuel cells (SOFCs) have been developed as clean and efficient power sources that generate electricity from various fuels. The SOFC has several distinct advantages, namely, simplicity, high power density, low production cost and excellent integration with a simple reformer. Thus, it is expected that their commercialization will be realized within a few years [1,2]. The fuel cell can be used as large power generator combined with gas turbine for stationary applications, a medium-sized power generator for residential applications with internally reformed fuel, and a small power generator for portable power applications. The SOFCs can be constructed with either a tubular or a planar design. The tubular design has been used for small to large-scale power generation systems. The planar design has also been studied for a long time and a small power system has been developed. To achieve commercialization of SOFC technology, it is essential to establish key technologies such

as cell components and a fabrication method for the tubular cell, a high performance cell, stack design and assembly, etc. In order to increase cell life and reduce cost through the use of less expensive materials such as metallic interconnects, many researchers are presently concentrating on the development of SOFCs which can operate at reduced temperatures below 800°C [2,3]. An anode-supported SOFC is a candidate for such intermediate-temperature system. Accordingly, we have investigated the characteristics of a cylindrical, anode-supported tube cell with a gastight electrolyte layer in previous work [4–6].

The present study is concerned with the development of an anode-supported flat-tube cell to improve power density and to study the basic technology of the key components, viz. electrode, electrolyte and interconnection materials.

2. Experimental procedure

2.1. Fabrication of anode-supported flat-tube cell

The extruded flat-tube anode support served as a fuel electrode. The other cell components were fabricated in

* Corresponding author. Tel.: +82-42-860-3578; fax: +82-42-860-3739.
E-mail address: rhsong@kier.re.kr (R.-H. Song).

thin layers and attached to the anode. A 40 vol.% Ni/YSZ (8 mol% yttria-stabilized zirconia) anode powder was prepared by mixing YSZ (TZ-8Y, Tosoh Co.) and nickel oxide powders. Anode powder and activated carbon as pore former were weighed and mixed in ethanol by ball milling for 14 days and then dried. An organic binder and 25 wt.% distilled water were added to the dried powder, and then the well-dispersed paste was extruded in the form of flat tube. The extruded flat tubes were dried with microwaves in an oven at 120 °C for 12 h, and then pre-sintered at 1300 °C. The YSZ electrolyte layer was coated on the pre-sintered anode tube by repeated application of a slurry dip process to form a dense layer, which was then co-fired at 1400 °C. The cathode materials $(\text{La}_{0.85}\text{Sr}_{0.15})_{0.9}\text{MnO}_3$ (LSM) and $\text{La}_{0.6}\text{Sr}_{0.4}\text{Co}_{0.2}\text{Fe}_{0.8}\text{O}_3$ (LSCF) were prepared by a solid-state powder reaction for which the materials were weighed in the required proportions and mixed in ethanol by ball milling for 10 days. The synthesized powder was calcined at 1000 °C for 5 h. The multi-layered cathode was composed of LSM/YSZ composite, LSM, and LSCF and was coated on to the co-sintered flat tube by a slurry dip process, and then sintered at 1200 °C. The pore size and porosity of the anode tube were determined by means of mercury porosimetry (Autopore IV 9500 V1.00, Micrometrics). The microstructure, thickness and elemental composition of the layers were evaluated by scanning electron microscopy (Philips model SEM515, USA) equipped with EDS and WDS. The performance characteristics of a single cell were evaluated at 750 °C in humidified hydrogen with 3% H_2O and air.

2.2. Fabrication of interconnection materials

Fecralloy (Fe–20Cr–5Al) and Fe–16Cr steel (SUS430, Changwon Special Steel Co., South Korea) of 3 mm thickness were used as metallic materials, and were polished with 600-grit SiC paper and cleaned in acetone. The metallic materials were dip-coated with the LSM slurry and sintered at 1200 °C for 2 h in two different atmospheres, viz. air and $\text{Ar} + 10\% \text{H}_2$. The electrical resistance was measured using the dc two-probe method and the interface layer was examined with scanning electron microscopy.

$\text{La}_{0.75}\text{Ca}_{0.27}\text{CrO}_3$ (LCC) as a ceramic interconnection material was synthesized from a nitrate solution of $\text{La}(\text{NO}_3)_3 \cdot 6\text{H}_2\text{O}$, $\text{Cr}(\text{NO}_3)_3 \cdot 6\text{H}_2\text{O}$ and $\text{Ca}(\text{NO}_3)_2 \cdot 4\text{H}_2\text{O}$ (Sigma–Aldrich). The nitrates were mixed with distilled water, and 1:1 molar mixture of ethylene glycol (EG) and citric acid (CA) was added to the solution. The solution was then heated to 80 °C on a hot plate to form a viscous gel. The resulting gel was put in a drying oven at 100 °C, and the solution was boiled rapidly to produce a polymerized foam. The gel was then dried and charred at 250 °C for 3 h. The charred resin was pulverized in a mortar. The precursors were calcined at each selected temperature in an air atmosphere, and the crystal phases of the calcined powders were identified by powder X-ray diffractometry (RINT

2000, Rigaku Co.). The LCC powder was plasma-sprayed on to the porous anode tube to form a gastight and electrically conducting interconnection. Plasma spray coating was carried out by using an arc-discharge, plasma spray gun (Sulzer Metco Co.). The spray-dried LCC agglomerates were fed into the plasma spray gun vertically by argon carrier gas and secondary H_2 , and then the plasma-coated LCC layer was heat-treated at 1400 °C for 3 h. The resulting layer was characterized by scanning electron microscopy. The characteristics of the plasma-sprayed ceramic interconnection layer were compared with those of the slurry dip-coated LCC layer with a NiO interlayer.

3. Results and discussion

3.1. Characteristics of anode-supported flat-tube cell

The extruded anode-supported flat-tube cell structure is shown in Fig. 1. The electron current path of the

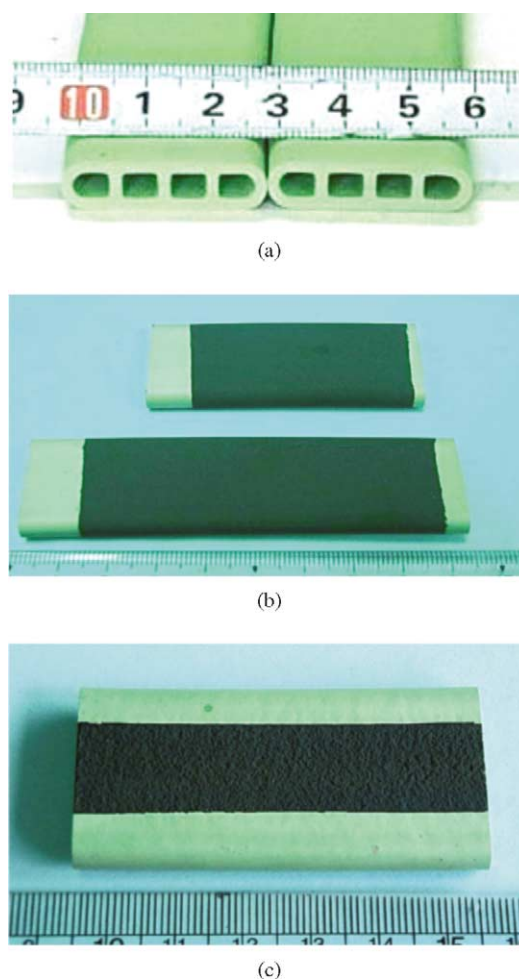


Fig. 1. Anode-supported flat-tube cells: (a) as-extruded and pre-sintered anode-supported flat tube; (b) flat-tube cell coated with electrolyte and cathode layer; (c) flat-tube cell coated with electrolyte and plasma spray-coated interconnect layer.

tubular-type SOFC structure is geometrically determined by the half-circle of the cell. Consequently, the power per mass or per volume is much poorer than that of the planar type. The flat-tube design can enhance the power density by providing electron current paths through the ribs, and shown in Fig. 1(a). The design also has higher mechanical strength than the conventional planar type. The flat-tube cell in which the electrolyte and the cathode layer are coated on the porous flat anode tube by slurry dip coating is shown in Fig. 1(b), and the plasma spray-coated interconnect layer on the anode tube is shown in Fig. 1(c). The thickness of the co-fired anode flat tube was 1.9 mm, and both the electrolyte and the cathode layers had a thickness of 20 μm .

The microstructure and elemental distribution of the anode-supported tube after reduction are shown in Fig. 2. The micrographs indicate a uniform distribution of Ni particles, YSZ, and micropores. Good distribution of the Ni

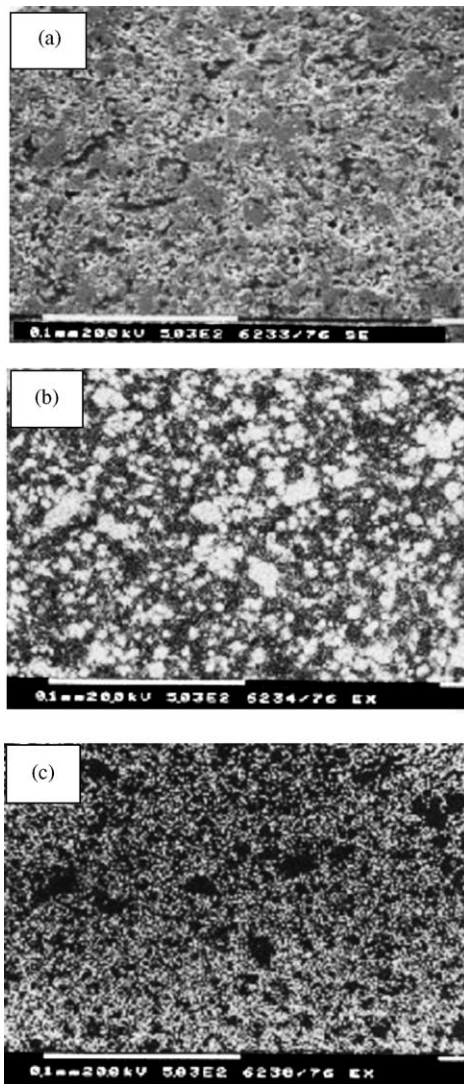


Fig. 2. Electron micrograph and elemental distribution of Ni and Zr(YSZ) in the Ni/YSZ cermet anode: (a) electron micrograph; (b) Ni K α X-ray image; (c) Zr L α X-ray image.

particles in the anode increases the number of electrode reaction sites by increasing the triple-phase boundary and current path [1]. The porosities of the anode tubes sintered at 1400 °C and pre-sintered at 1300 °C were 50.2 and 42.1%, respectively. A higher sintering temperature produces a lower porosity due to increased shrinking. After hydrogen reduction, the NiO in the anode tube is fully reduced to Ni and the porosity of the sintered anode tube is increased from 42.1 to 50.7%, which is considered to be caused by the volume change due to conversion of the nickel oxide to its metallic form.

The microstructure and elemental distributions of the electrolyte and the cathode multi-layer composed of LSM/40 wt.% YSZ composite, LSM and LSCF are presented in Fig. 3. The LSM/YSZ composite layer was adapted to a lower polarization loss due to an increase in the triple-phase (LSM/YSZ/gas) boundary [7]. The coated cathode layers were porous and the Mn in the LSM was diffused into the LSCF layer. The Fe in the LSCF was diffused slightly into the LSM layer, but mainly existed

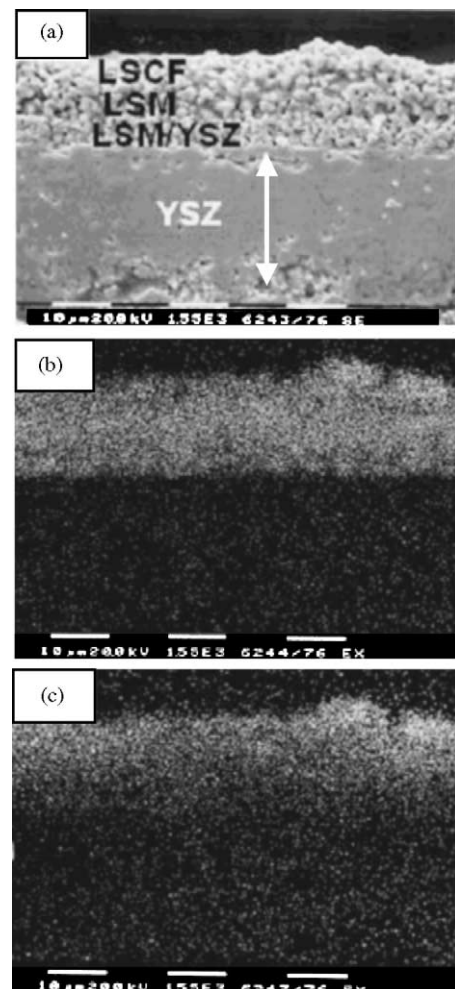


Fig. 3. Electron micrograph and elemental distribution of Mn and Fe of flat-tube cell: (a) electron micrograph; (b) Mn K α X-ray image; (c) Fe K α X-ray image.

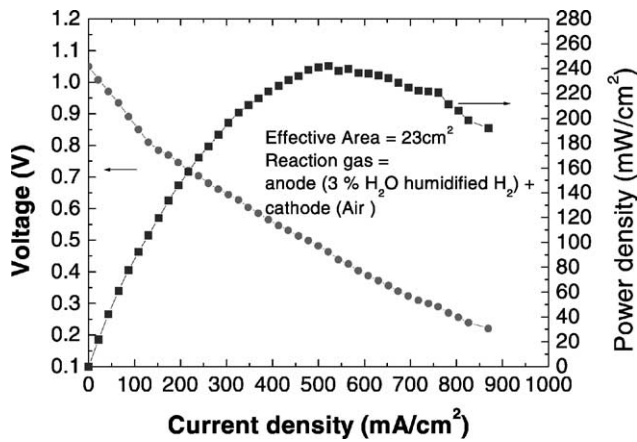


Fig. 4. Performance curves of flat-tube cell effective area of 23 cm² at 750 °C.

in the LSCF layer. Since Mn is the electrocatalytic reaction site, the diffused Mn exerts an influence on cathode performance. In the present work, it is unclear whether the diffused Mn increased the cathode activity or not. An anode-supported flat-tube cell with an effective cell area of 23 cm² produces a good performance of 225 mW cm⁻² (0.6 V, 375 mA cm⁻²) at 750 °C, as shown in Fig. 4. By contrast, a flat cell without a LSCF layer gave an inferior performance. A LSCF current-collector layer was coated on the LSM layer. LSCF has high electronic conductivity and therefore reduces the contact resistance of the cathode component.

3.2. Characteristics of metallic interconnector

The use of a metallic interconnector in a SOFC has the advantages of higher electronic conductivity and better workability at intermediate operating temperatures. There have been some studies on the use of metallic alloys as interconnectors [8–11]. These focused on studying the oxidation resistance, the electrical conductivity and the microstructure of Fe- and Cr-based alloys [10,12,13]. To examine the effect of the LSM slurry coating on the metallic alloy, Fecralloy (Fe–20Cr–5Al) and Fe–16Cr alloy were coated with a (La_{0.85}Sr_{0.15})_{0.9}MnO₃ protective layer by a dipping process and the characteristics of the interface layer and the electronic conductivity were investigated.

When the LSM-coated Fe–16Cr alloy was sintered in an Ar + 10% H₂ atmosphere, the coating layer had a thickness of about 30 μm and was stable; a cross-section of this layer is shown in Fig. 5. At the interface layer of Fe–16Cr alloy and LSM, Cr₂O₃ phase is detected from the composition analysis and the dense LSM layer is strongly bonded to metal substrate.

On the other hand, the LSM layer sintered in an air atmosphere delaminated from the metal substrate. This is attributed to the formation of thick oxide scale at the interface of the Fe–16Cr alloy/LSM layer. In the case of Fecralloy,

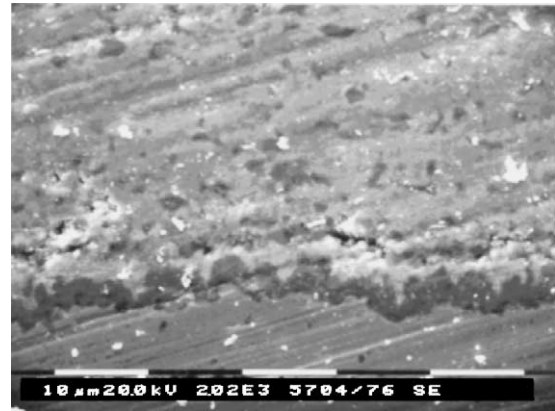


Fig. 5. Electron micrograph of Fe–16Cr alloy (SUS430)/LSM interface sintered in Ar + 10% H₂.

delamination of the LSM coating layer did not occur in an air-sintered condition, which is probably due to the formation of an adherent Al₂O₃ or mixed Al₂O₃ protective layer. The total electrical resistance of LSM-coated Fecralloy is higher than that of Fe–16Cr, as shown in Fig. 6(a), and is caused by the presence of Al₂O₃ with low conductivity in the Fecralloy. Total electrical resistance of Fe–16Cr alloy

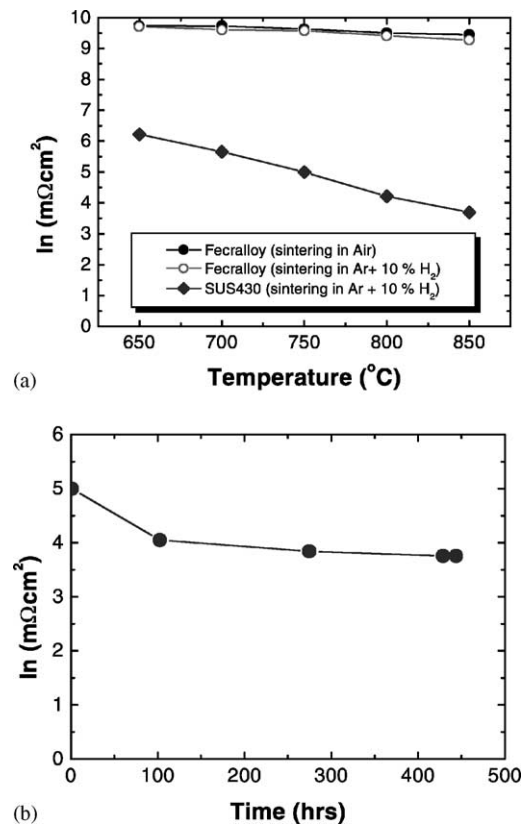


Fig. 6. (a) Electrical resistance of Fe–16Cr alloy (SUS430) and Fecralloy coated with LSM. (b) Variation of electrical resistance as a function of holding time.

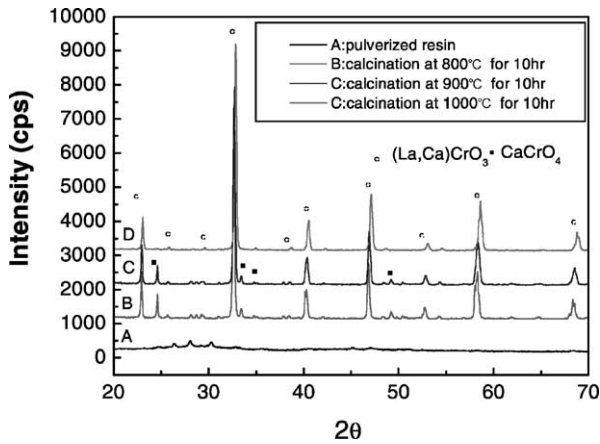


Fig. 7. XRD patterns of synthesized $\text{La}_{0.75}\text{Ca}_{0.27}\text{CrO}_3$ powder as a function of calcination temperature.

as a function of time is presented in Fig. 6(b). The value is $148 \text{ m}\Omega \text{ cm}^2$ at 750°C and decreases to $43 \text{ m}\Omega \text{ cm}^2$ after 450 h, which is considered to be due to the LSM coating layer changing to stable single phase [10]. This result confirms the suitability of the metallic interconnect for anode-supported flat-tube SOFCs.

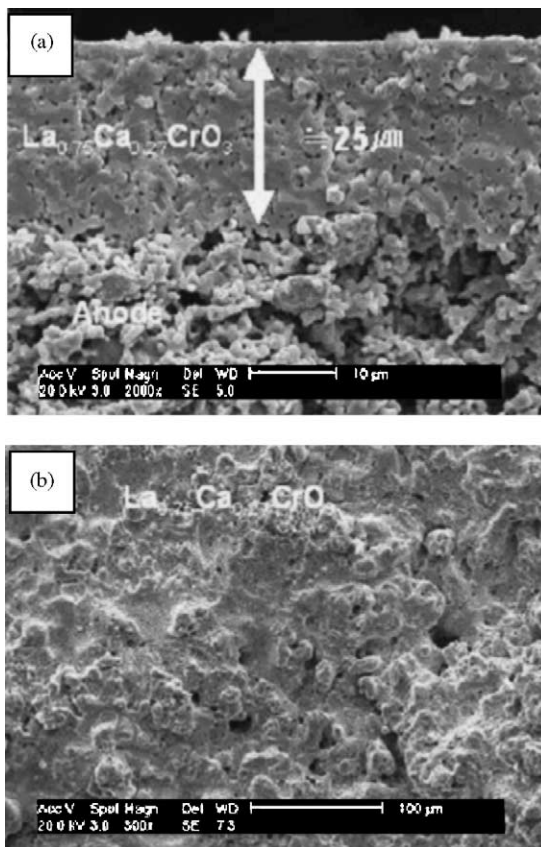


Fig. 8. Electron micrograph of plasma spray-coated and sintered $\text{La}_{0.75}\text{Ca}_{0.27}\text{CrO}_3$ at 1400°C for 3 h: (a) cross-section of coated layer; (b) surface of coated layer.

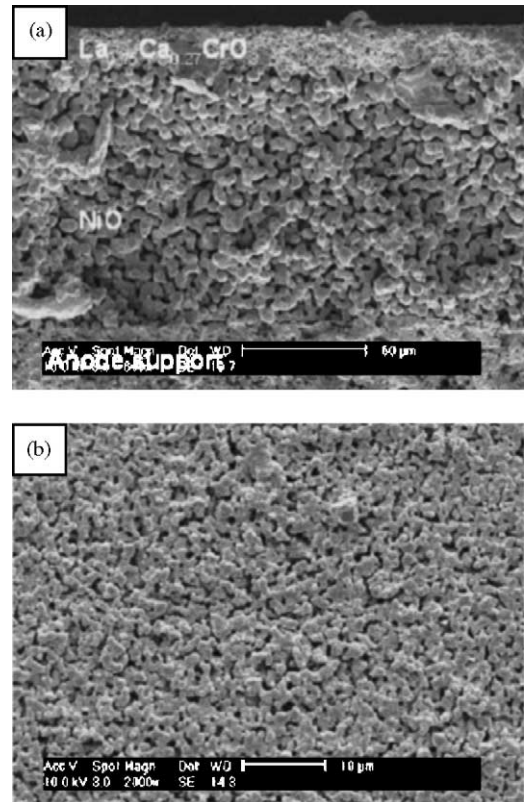


Fig. 9. Slurry dip-coated and sintered $\text{La}_{0.75}\text{Ca}_{0.27}\text{CrO}_3$ at 1400°C for 3 h. NiO coated as barrier layer: (a) cross-section of coated layer; (b) surface of coated layer.

3.3. Characteristics of ceramic interconnect coated on anode-supported tube

X-ray diffraction patterns of $\text{La}_{0.75}\text{Ca}_{0.27}\text{CrO}_3$ samples calcined at different temperatures are shown in Fig. 7. A second phase, CaCrO_4 , is found in addition to the main perovskite phase in samples calcined at 800 and 900°C for 10 h. The single phase of perovskite is present at temperatures above 1000°C . The powders were made in the form of a spherical shape by a spray drying process. The powder was fed into a plasma spray gun via argon carrier gas, melted by the plasma arc, and deposited on the anode-supported flat tube to form a ceramic interconnection film. To improve the gas tightness, the anode tube with the plasma-sprayed film was heated-treated at 1400°C in air for 3 h. The results are presented in Fig. 8 and the plasma-sprayed thin layer was dense. To provide a comparison with the wet process, $\text{La}_{0.75}\text{Ca}_{0.27}\text{CrO}_3$ slurry was dip-coated on the anode support coated with NiO layer. The dense interconnection layer was not formed, as shown in Fig. 9.

4. Conclusions

In order to increase the cell power density and thermal stability through a combination of tubular and planar cell

structures, an anode-supported flat-tube solid oxide fuel cells has been developed. The anode-supported flat tube was successfully fabricated by an extrusion process, and is coated with a ceramic interconnection film in the form of a band. The flat cells are connected electrically by the ceramic film and a metallic plate. A dense electrolyte layer and a porous cathode layer were coated on the anode tube subsequently by slurry dip coating process. The anode-supported flat-tube cell shows a good performance of 225 mW cm^{-2} (0.6 V , 375 mA cm^{-2}) at 750°C . For a flat-tube cell stack, a commercial metallic interconnection plate with a LSM layer was developed, which shows a low and stable electrical resistance of $43 \text{ m}\Omega \text{ cm}^2$ after 450 h due probably to a phase change in the LSM layer. Construction of a stack composed of flat cells and metallic interconnection plates is in progress.

References

- [1] N.Q. Minh, T. Takahashi, Science and Technology of Ceramic Fuel Cell, Elsevier, Amsterdam, 1995.
- [2] K. Huang, M. Feng, J.B. Goodenough, J. Am. Ceram. Soc. 81 (1998) 357–362.
- [3] P. Charpentier, P. Fragnaud, D.M. Schleich, E. Gehain, Solid State Ionics 135 (2000) 373–380.
- [4] R.-H. Song, E.Y. Kim, D.R. Shin, H. Yokokawa, in: U. Stimming, S.C. Singhal, H. Tagwa (Eds.), Proceedings of the Sixth International Symposium on Solid Oxide Fuel Cells, vol. 99-19, The Electrochemical Society, Pennington, NJ, USA, 1999, pp. 845–850.
- [5] R.-H. Song, K.-S. Song, Y.E. Ihm, H. Yokokawa, in: H. Yokokawa, S.C. Singhal (Eds.), Proceedings of the Seventh International Symposium on Solid Oxide Fuel Cells, 2001-16, The Electrochemical Society, Pennington, NJ, USA, 2001, pp. 1073–1079.
- [6] K.-S. Song, R.-H. Song, Y.E. Ihm, Korean J. Mater. Sci. 12 (2002) 691–695.
- [7] S. Wang, et al., J. Electrochem. Soc. 145 (1998) 1932–1939.
- [8] W. Thierfelder, H. Greiner, W. Kock, in: Proceedings of the Fifth International Symposium on Solid Oxide Fuel Cells, Pennington, NJ, USA, 1997, pp. 1306–1315.
- [9] P. Kofstad, R. Bredesen, Solid State Ionics 52 (1992) 69–75.
- [10] J.Q. Li, P. Xiao, J. Eur. Ceram. Soc. 21 (2001) 659–668.
- [11] B. Tomasz, N. Makoto, M. Toshi, P. Kazimierz, Solid State Ionics 143 (2001) 131–150.
- [12] S. Linderoth, P.V. Hendriksen, M. Mogensen, N. Langvad, J. Mater. Sci. 31 (1996) 5077–5082.
- [13] W.J. Quadackers, H. Greiner, M. Hansel, A. Pattanaik, A.S. Khanna, W. Mallener, Solid State Ionics 91 (1996) 55–67.